MicroRNAs from the parasitic plant *Cuscuta campestris* target host messenger RNAs

Saima Shahid[1,2], Gunjune Kim[3], Nathan R. Johnson[1,2], Eric Wafula[2], Feng Wang[1,2,4], Ceyda Coruh[1,2,5], Vivian Bernal-Galeano[3], Tamia Phifer[6], Claude W. dePamphilis[1,2], James H. Westwood[3], and Michael J. Axtell[1,2]

[1] Intercollege Ph.D. Program in Plant Biology, Huck Institutes of the Life Sciences, The Pennsylvania State University, University Park, PA 16802 USA

[2] Department of Biology, The Pennsylvania State University, University Park, PA 16802 USA

[3] Department of Plant Pathology, Physiology and Weed Science, Virginia Polytechnic Institute and State University, Blacksburg, VA 24061, USA.

[4] Current Address: Department of Biology, Indiana University, Bloomington IN 47405, USA

[5] Current Address: Salk Institute for Biological Studies, La Jolla, CA 92037, USA

[6] Knox College, Galesburg, IL 61401, USA

First paragraph:

Dodders (*Cuscuta* spp.) are obligate parasitic plants that obtain water and nutrients from the stems of host plants via specialized feeding structures called haustoria. Dodder haustoria facilitate bi-directional movement of viruses, proteins, and mRNAs between host and parasite[1], but the functional effects of these movements are

24 not clear. Here we show that *C. campestris* haustoria accumulate high levels of many
25 novel microRNAs (miRNAs) while parasitizing *Arabidopsis thaliana* hosts. Many of
26 these miRNAs are 22 nts long, a usually rare size of plant miRNA associated with
27 amplification of target silencing through secondary small interfering RNA (siRNA)
28 production[2]. Several *A. thaliana* mRNAs are targeted by *C. campestris* 22 nt miRNAs
29 during parasitism, resulting in mRNA cleavage, secondary siRNA production, and
30 decreased mRNA accumulation levels. Hosts with mutations in two of the targets
31 supported significantly higher growth of *C. campestris.* Homologs of target mRNAs from
32 diverse plants also have predicted target sites to induced *C. campestris* miRNAs, and
33 the same miRNAs are expressed and active against host targets when *C. campestris*
34 parasitizes a different host, *Nicotiana benthamiana*. These data show that *C. campestris*
35 miRNAs act as *trans*-species regulators of host gene expression, and suggest that they
36 may act as virulence factors during parasitism.
37
38 Host-induced gene silencing (HIGS) involves plant transgenes that produce
39 siRNAs which can silence targeted pathogen/parasite mRNAs in *trans*[3,4]. Plant-based
40 HIGS is effective against fungi[5], nematodes[6], insects[7], and the parasitic plant *Cuscuta*
41 *pentagona*[8]. The apparent ease of engineering HIGS suggests that plants might
42 exchange naturally occurring small RNAs during pathogen/parasite interactions.
43 Consistent with this hypothesis, small RNAs from the plant pathogenic fungus *Botrytis*
44 *cinerea* target host mRNAs during infection[9], and HIGS targeting *B. cinerea Dicer-Like*
45 mRNAs reduces pathogen virulence[10]. Conversely, the conserved miRNAs miR159 and
46 miR166 can be exported from cotton into the fungal pathogen *Verticillium dahliae* where

47 they target fungal mRNAs encoding virulence factors[11]. However, to date, no examples
48 of naturally occurring *trans*-species miRNAs have been described for plant-to-plant
49 interactions.

50 *Cuscuta* haustoria facilitate bi-directional movement of viruses, proteins, and
51 mRNAs[1], but the functional effects of these movements are unclear. *Cuscuta* is
52 susceptible to HIGS, so we hypothesized that naturally occurring small RNAs might be
53 exchanged across the *C. campestris* haustorium and affect gene expression in the
54 recipient species. To test this hypothesis, we profiled small RNA expression from *C.*
55 *campestris* grown on *A. thaliana* hosts using high-throughput small RNA sequencing
56 (sRNA-seq). Two biological replicates each from three tissues were analyzed: Parasite
57 stem (PS), comprising a section of *C. campestris* stem above the site of haustorium
58 formation; Interface (I), comprising *C. campestris* stem with haustoria with associated *A.*
59 *thaliana* stem tissue; and Host stem (HS), comprising sections of *A. thaliana* stems
60 above the interface region, as previously described[12]. Small RNA-producing loci from
61 both organisms were identified, classified, and subject to differential expression
62 analyses (Supplementary Data 1).
63

64 As expected due to dilution of parasite RNA with host RNA, *C. campestris* small
65 RNA loci were generally down-regulated in I relative to PS (Figure 1A). However, 76 *C.*
66 *campestris* small RNA loci were significantly (FDR <= 0.05) higher in I relative to PS. 43
67 of these (57%) were *MIRNA* loci as determined by canonical accumulation of a discrete
68 miRNA/miRNA* pair from predicted stem-loop precursors (Figure 1B, Supplementary
69 Data 2-4). RNA blots confirmed I-specific expression (Figure 1C). One of the 43

70 *MIRNA*s is a member of the conserved *MIR164* family; the other 42 up-regulated
71 *MIRNA*s have no obvious sequence similarity to previously annotated *MIRNA* loci, and
72 none of their mature miRNAs or miRNA*s were perfectly alignable to the *A. thaliana*
73 genome (Supplementary Data 5). Several of the key *MIRNA* loci were detected by PCR
74 of *C. campestris* genomic DNA prepared from four-day old seedlings that had never
75 interacted with a host plant (Extended Data Figure 1). The majority of the induced *C.*
76 *campestris MIRNA* loci (26/43) produced a 22 nt mature miRNA. 22 nt plant miRNAs
77 are usually less frequent than 21nt miRNAs, and they are strongly associated with
78 secondary siRNA accumulation from their targets[13,14]. Secondary siRNAs are thought to
79 amplify the strength of miRNA-directed gene silencing[2].
80
81 ----------

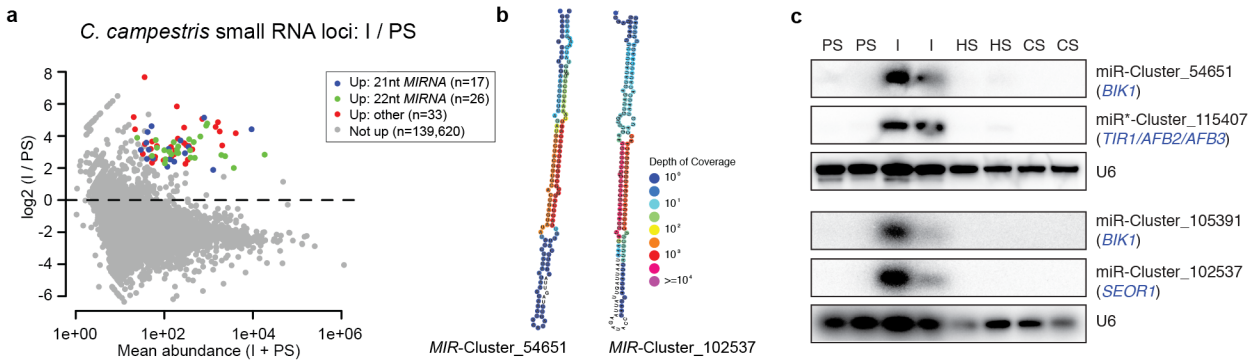

82
83
84 **Figure 1**. *C. campestris* miRNAs induced at the haustorial interface. **a)** MA plot of *C.*
85 *campestris* small RNA loci comparing interface (I) to parasite stem (PS) samples.
86 Significantly up-regulated loci (alternative hypothesis: true difference > 2-fold, FDR <=
87 0.05) are highlighted. **b)** Predicted secondary structures of example *MIRNA* hairpin
88 precursors of *C. campestris* 22 nt miRNAs. Color-coding shows depth of small RNA-seq

89 coverage at each nucleotide. **c)** RNA blots of 22 nt I-induced miRNAs. PS: parasite
90 stem, I: interface, HS: host stem, CS: control stem.
91 ----------
92 We hypothesized that the induced 22 nt miRNAs would cause secondary siRNA
93 formation from targeted host mRNAs. Therefore we searched for *A. thaliana* mRNAs
94 that had one or more plausible miRNA complementary sites and accumulation of
95 secondary siRNAs specifically in the I small RNA-seq samples. Six *A. thaliana* mRNAs
96 that met both criteria were found: *TIR1*, *AFB2*, and *AFB3*, which encode related and
97 partially redundant auxin receptors[15], *BIK1*, which encodes a plasma membrane-
98 localized kinase required for both pathogen-induced and developmental signaling[16,17],
99 *SEOR1*, which encodes a major phloem protein that accumulates in filamentous
100 networks in sieve tube elements and reduces photosynthate loss from the phloem upon
101 injury[18,19], and *SCZ/HSFB4*, which encodes a predicted transcriptional repressor that is
102 required for the formation of ground tissue stem cells in roots[20-22]. The induced siRNAs
103 from these mRNAs resembled other examples of secondary siRNAs in their size
104 distributions, double-stranded accumulation, and phasing (Figure 2A-B; Extended Data
105 Figure 2). *TIR1*, *AFB2*, and *AFB3*, are also known to be targeted by the 22 nt miR393
106 and to produce secondary siRNAs downstream of the miR393 complementary site[23]. In
107 parasitized stems the location and phase register of the *TIR1*, *AFB2*, and *AFB3*
108 secondary siRNAs shift upstream, proximal to the complementary sites to the *C.*
109 *campestris* miRNAs (Extended Data Figure 2), implying that the *C. campestris* miRNAs,
110 not miR393, are triggering the I-specific secondary siRNAs. The predominant 21 nt
111 phase register at several loci was shifted +1 to +2 relative to the predictions. This is

consistent with the 'phase drift' seen at other phased siRNA loci[24,25] and likely due to the presence of low levels of 22nt siRNAs, causing the register to be shifted forward. Analysis of uncapped mRNA fragments using 5'-RNA ligase-mediated rapid amplification of cDNA ends found strong evidence for miRNA-directed cleavage at all of the complementary sites to *C. campestris* miRNAs, specifically from interface samples but not from control stem samples (Figure 2; Extended Data Figure 2). We did not find any induced miRNAs or siRNAs from the *A. thaliana* host capable of targeting these six mRNAs. We also did not find any endogenous *C. campestris* secondary siRNA loci corresponding to any of the induced miRNAs. Some *C. campestris* orthologs of *TIR/AFB, SCZ/HSFB4*, and *BIK1* had possible, but very poorly complementary, miRNA target sites (Extended Data Figure 3). These observations suggest that the induced *C. campestris* miRNAs have evolved to avoid targeting 'self' transcripts. We conclude that 22 nt miRNAs from *C. campestris* act in a *trans*-species manner to target *A. thaliana* mRNAs.

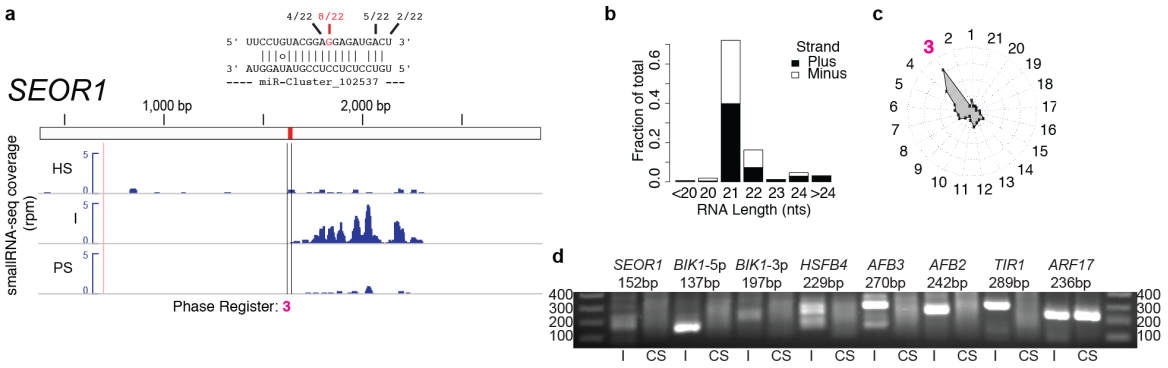

Figure 2. *C. campestris* miRNAs cause slicing and phased siRNA production from host mRNAs. **a)** Small RNA-seq coverage (reads per million) for the *A. thaliana SEOR1*

131 transcript for host stem (HS), interface (I), and parasite stem (PS) samples. miRNA
132 complementary site with 5'-RLM-RACE data and expected 21nt phasing register is
133 shown. **b)** Length and polarity distribution of *SEOR1*-mapped siRNAs from the I
134 samples. **c)**. Radar chart showing fraction of I-derived siRNAs in each of the 21
135 possible phasing registers. **d)** 5'-RLM-RACE products from nested amplifications for the
136 indicated cDNAs. I: interface, CS: control stem. *ARF17* is a positive control.
137 ----------
138
139 Accumulation of five of the six secondary siRNA-producing targets was
140 significantly reduced in stems parasitized by *C. campestris* compared to un-parasitized
141 stems (Figure 3A), consistent with miRNA-mediated repression. The true magnitude of
142 repression for these targets could be even greater, since many miRNAs also direct
143 translational repression. Accumulation of many known *A. thaliana* secondary siRNAs is
144 often partially dependent on the endonuclease Dicer-Like 4 (DCL4) and wholly
145 dependent on RNA-Dependent RNA polymerase 6 (RDR6/SGS2/SDE1)[2]. Accumulation
146 of an abundant secondary siRNA from *TIR1* was eliminated entirely in the *sgs2-1*
147 mutant, and reduced in the *dcl4-2t* mutant (Figure 3B). Thus host *DCL4* and
148 *RDR6/SGS2/SDE1* are required for secondary siRNA production. This implies that the
149 *C. campestris* derived miRNAs are active inside of host cells and hijack the host's own
150 silencing machinery to produce secondary siRNAs.
151 In repeated trials with varying methodologies we did not observe consistent
152 significant differences in parasite fresh weight using *dcl4-2t* and *sgs2-1* mutants as
153 hosts (Extended Data Figure 4). Thus, loss of induced secondary siRNAs is not

154 sufficient to detectably affect parasite biomass accumulation in this assay. Similarly,
155 there were no significant differences in parasite fresh weights when *scz2* or *tir1-1/afb2-3*
156 plants were used as hosts (Figure 3C). Significantly less *C. campestris* biomass was
157 observed using *bik1* mutants as hosts. However, interpretation of this result is
158 complicated by the weak, frequently lodging stems of the *bik1* mutant[16]. Significantly
159 more *C. campestris* biomass was observed when grown on *seor1* or *afb3-4* mutant
160 hosts (Figure 3C). Therefore, both *SEOR1* and *AFB3* function to restrict *C. campestris*
161 growth on *A. thaliana*. This observation is consistent with the hypothesis that both
162 *SEOR1* and *AFB2* are *trans*-species miRNA targets of biological relevance.
163
164 ----------

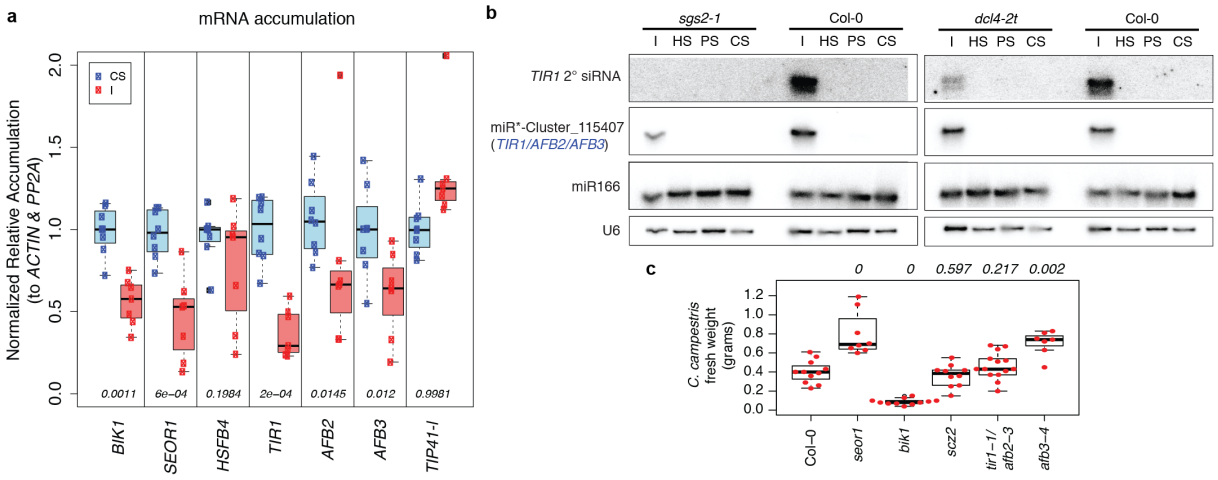

165

166 **Figure 3**. Effects of *C. campestris* miRNAs and their targets. **a)** *A. thaliana* mRNA
167 accumulation levels in I (interface) vs. CS (control stems) during *C. campestris*
168 parasitism, assessed by qRT-PCR. Data from 7 or 8 biological replicates are plotted
169 (dots), and boxplots indicate the median (horizontal lines), 1st-3rd quartile range
170 (boxes), and up to 1.5 x the interquartile range (whiskers). Numbers indicate p-values
171 comparing CS and I samples (Wilcoxon rank-sum test, unpaired, one-tailed). *TIP41-I* :

172 control mRNA. **b)** RNA blots from *C. campestris* infestations of the indicated *A. thaliana*
173 genotypes. I: interface, HS: host stem, PS: parasite stem, CS: control stem. **c)**
174 Accumulation of *C. campestris* biomass on *A. thaliana* hosts of the indicated genotypes
175 18 days post-attachment. P-values (Wilcoxon rank-sum tests, unpaired, two-tailed) from
176 comparison of mutant to wild-type (Col-0) are shown. Boxplot conventions as in panel a.
177 n=11, 8, 11, 10, 14, and 7 for Col-0, *seor1*, *bik1, scz2, tir1-1/afb2-3*, and *afb3*,
178 respectively.
179 ----------
180 *C. campestris* has a broad host range among eudicots[26]. Therefore, we searched
181 for miRNA complementary sites for the interface-induced *C. campestris* miRNAs in
182 eudicot orthologs of the targeted *A. thaliana* mRNAs. Probable orthologs of *BIK1,*
183 *SEOR1, TIR/AFB*, and *SCZ/HSFB4* were predicted targets of interface-induced miRNAs
184 in many eudicot species, while only one species had predicted targets for the negative
185 control orthologs of *GAPDH* (Figure 4A, Extended Data Table 1). We conclude that the
186 induced *C. campestris* miRNAs collectively would be able to target *TIR/AFB, SEOR1,*
187 *SCZ/HSFB4*, and *BIK1* orthologs in many eudicot species.
188 We performed additional small RNA-seq from *C. campestris* on *A. thaliana* hosts,
189 and from *C. campestris* on *Nicotiana benthamiana* hosts. Both sets of experiments were
190 designed identically to the original small RNA-seq study (two biological replicates each
191 of HS, I, and PS samples). The I-induced set of *C. campestris MIRNA* loci was highly
192 reproducible across both of the *A. thaliana* experiments as well as the *N. benthamiana*
193 experiment (Extended Data Figure 5). Induction of several *C. campestris* miRNAs
194 during *N. benthamiana* parasitism was confirmed by RNA blots (Figure 4B). Several *N.*

benthamiana mRNAs had both plausible target sites for *C. campestris* miRNAs and accumulation of phased, secondary siRNAs in the I samples, including orthologs of *TIR/AFB* and *BIK1* (Extended Data Figure 6). Analysis of uncapped RNA ends provided strong evidence for miRNA-directed cleavage of one of the *N. benthamiana TIR1/AFB* orthologs (Figures 4C-D; Extended Data Figure 7). This directly demonstrates that the same *C. campestris* miRNAs target orthologous host mRNAs in multiple species. None of the interface-induced miRNAs we tested were detectable from *C. campestris* pre-haustoria sampled from seedling tips that had coiled around dead bamboo stakes instead of a live host (Figure 4B; Extended Data Figure 8). This suggests that expression of these miRNAs requires prior contact with a living host.

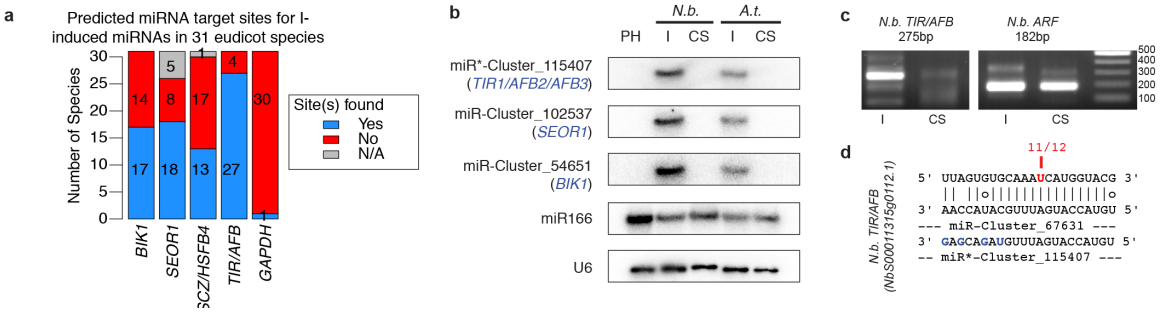

Figure 4. Conservation of host mRNA targeting by *C. campestris*. **a)** Predicted targets of the induced *C. campestris* miRNAs/miRNA*s among indicated orthologs. **b)** RNA blots from interface (I) and control stem (CS) samples of *C. campestris* infested *N. benthamiana* (*N.b.*) and *A. thaliana* (*A.t.*) hosts, as well as *C. campestris* pre-haustoria (PH; Extended Data Figure 8). **c)** 5'-RLM-RACE products for the indicated *N. benthamiana* cDNAs. I: interface, CS: control stem. *N.b. ARF* is a positive control. Image cropped to remove irrelevant lanes; uncropped image: Extended Data Figure 7.

214 **d)** Complementary site and 5'-RLM-RACE results from a *N. benthamiana TIR/AFB*
215 ortholog.
216 ----------
217
218 These data demonstrate that *C. campestris* induces a large number of miRNAs
219 at the haustorium, and that some of them target host mRNAs and reduce their
220 accumulation. Many of the induced miRNAs are 22 nts long, and associated with
221 secondary siRNA production from their host targets using the host's own secondary
222 siRNA machinery. Several of the targets are linked to plant pathogenesis: Manipulation
223 of *TIR1/AFB2/AFB3* accumulation levels affects bacterial pathogenesis and defense
224 signaling[27], and BIK1 is a central regulator of pathogen-induced signaling[28]. Perhaps
225 the most intriguing target is *SEOR1*, which encodes a very abundant protein present in
226 large agglomerations in phloem sieve-tube elements[18]. *seor1* mutants have an
227 increased loss of sugars from detached leaves[19], and our data show that *seor1* mutants
228 also support increased *C. campestris* biomass accumulation. A key function of the
229 haustorium is to take nutrients from the host phloem; targeting *SEOR1* could be a
230 strategy to increase sugar uptake from host phloem. Overall, these data suggest that *C.*
231 *campestris trans*-species miRNAs might function as virulence factors to remodel host
232 gene expression to its advantage during parasitism.
233
234 **Methods** [separate online only document].
235
236 **References**

237 1. Kim, G. & Westwood, J. H. Macromolecule exchange in Cuscuta-host plant
238 interactions. *Curr Opin Plant Biol* **26,** 20–25 (2015).
239 2. Fei, Q., Xia, R. & Meyers, B. C. Phased, Secondary, Small Interfering RNAs in
240 Posttranscriptional Regulatory Networks. *Plant Cell* **25,** 2400–2415 (2013).
241 3. Baulcombe, D. C. VIGS, HIGS and FIGS: small RNA silencing in the interactions
242 of viruses or filamentous organisms with their plant hosts. *Curr Opin Plant Biol* **26,**
243 141–146 (2015).
244 4. Weiberg, A., Bellinger, M. & Jin, H. Conversations between kingdoms: small
245 RNAs. *Curr. Opin. Biotechnol.* **32,** 207–215 (2015).
246 5. Nowara, D. *et al.* HIGS: host-induced gene silencing in the obligate biotrophic
247 fungal pathogen Blumeria graminis. *Plant Cell* **22,** 3130–3141 (2010).
248 6. Huang, G., Allen, R., Davis, E. L., Baum, T. J. & Hussey, R. S. Engineering broad
249 root-knot resistance in transgenic plants by RNAi silencing of a conserved and
250 essential root-knot nematode parasitism gene. *Proc Natl Acad Sci USA* **103,**
251 14302–14306 (2006).
252 7. Baum, J. A. *et al.* Control of coleopteran insect pests through RNA interference.
253 *Nat Biotechnol* **25,** 1322–1326 (2007).
254 8. Alakonya, A. *et al.* Interspecific RNA interference of SHOOT MERISTEMLESS-
255 like disrupts Cuscuta pentagona plant parasitism. *Plant Cell* **24,** 3153–3166
256 (2012).
257 9. Weiberg, A. *et al.* Fungal small RNAs suppress plant immunity by hijacking host
258 RNA interference pathways. *Science* **342,** 118–123 (2013).
259 10. Wang, M. *et al.* Bidirectional cross-kingdom RNAi and fungal uptake of external

260 RNAs confer plant protection. *Nature Plants* **2,** 16151 (2016).
261 11. Zhang, T. *et al.* Cotton plants export microRNAs to inhibit virulence gene
262 expression in a fungal pathogen. *Nature Plants* **2,** 16153 (2016).
263 12. Kim, G., LeBlanc, M. L., Wafula, E. K., dePamphilis, C. W. & Westwood, J. H.
264 Plant science. Genomic-scale exchange of mRNA between a parasitic plant and
265 its hosts. *Science* **345,** 808–811 (2014).
266 13. Chen, H.-M. *et al.* 22-Nucleotide RNAs trigger secondary siRNA biogenesis in
267 plants. *Proc Natl Acad Sci USA* **107,** 15269–15274 (2010).
268 14. Cuperus, J. T. *et al.* Unique functionality of 22-nt miRNAs in triggering RDR6-
269 dependent siRNA biogenesis from target transcripts in Arabidopsis. *Nat Struct*
270 *Mol Biol* **17,** 997–1003 (2010).
271 15. Dharmasiri, N. *et al.* Plant development is regulated by a family of auxin receptor
272 F box proteins. *Dev Cell* **9,** 109–119 (2005).
273 16. Veronese, P. *et al.* The membrane-anchored BOTRYTIS-INDUCED KINASE1
274 plays distinct roles in Arabidopsis resistance to necrotrophic and biotrophic
275 pathogens. *Plant Cell* **18,** 257–273 (2006).
276 17. Lin, W. *et al.* Inverse modulation of plant immune and brassinosteroid signaling
277 pathways by the receptor-like cytoplasmic kinase BIK1. *Proc Natl Acad Sci USA*
278 **110,** 12114–12119 (2013).
279 18. Froelich, D. R. *et al.* Phloem ultrastructure and pressure flow: Sieve-Element-
280 Occlusion-Related agglomerations do not affect translocation. *Plant Cell* **23,**
281 4428–4445 (2011).
282 19. Jekat, S. B. *et al.* P-proteins in Arabidopsis are heteromeric structures involved in

283 rapid sieve tube sealing. *Front Plant Sci* **4,** 225 (2013).
284 20. Mylona, P., Linstead, P., Martienssen, R. & Dolan, L. SCHIZORIZA controls an
285 asymmetric cell division and restricts epidermal identity in the Arabidopsis root.
286 *Development* **129,** 4327–4334 (2002).
287 21. Pernas, M., Ryan, E. & Dolan, L. SCHIZORIZA controls tissue system complexity
288 in plants. *Curr Biol* **20,** 818–823 (2010).
289 22. Hove, ten, C. A. *et al.* SCHIZORIZA encodes a nuclear factor regulating
290 asymmetry of stem cell divisions in the Arabidopsis root. *Curr Biol* **20,** 452–457
291 (2010).
292 23. Si-Ammour, A. *et al.* miR393 and secondary siRNAs regulate expression of the
293 TIR1/AFB2 auxin receptor clade and auxin-related development of Arabidopsis
294 leaves. *Plant Physiol* **157,** 683–691 (2011).
295 24. Allen, E., Xie, Z., Gustafson, A. M. & Carrington, J. C. microRNA-Directed
296 Phasing during Trans-Acting siRNA Biogenesis in Plants. *Cell* **121,** 207–221
297 (2005).
298 25. Axtell, M. J., Jan, C., Rajagopalan, R. & Bartel, D. P. A two-hit trigger for siRNA
299 biogenesis in plants. *Cell* **127,** 565–577 (2006).
300 26. Dawson, J. H., Musselman, L. J., Wolswinkel, P. & Dörr, I. Biology and control of
301 Cuscuta. *Reviews of Weed Science* **6,** 265–317 (1994).
302 27. Robert-Seilaniantz, A. *et al.* The microRNA miR393 re-directs secondary
303 metabolite biosynthesis away from camalexin and towards glucosinolates. *Plant J*
304 **67,** 218–231 (2011).
305 28. Lu, D. *et al.* A receptor-like cytoplasmic kinase, BIK1, associates with a flagellin

306 receptor complex to initiate plant innate immunity. *Proc Natl Acad Sci USA* **107,**
307 496–501 (2010).
308

309 **Acknowledgements**

310 We thank the Penn State & Huck Institutes Genomics Core Facility for small RNA-seq
311 services. We thank Hervé Vaucheret, Michael Knoblauch, Gabriele Monshausen,
312 Tesfaye Mengiste, and Renze Heidstra for gifts of *A. thaliana* mutant seed. We thank
313 Beth Johnson for advice on growing conditions for *C. campestris*. Purchase of the
314 Illumina HiSeq2500 used for small RNA-seq was funded by a major research
315 instrumentation award from the US National Science Foundation [1229046 to MJA and
316 CWD]. This research was supported in part by awards from the US National Science
317 Foundation [1238057 to JHW and CWD; 1339207 to MJA] and the National Institute of
318 Food and Agriculture [135997 to JHW].
319

320 **Author Contributions**: SS and MJA performed most bioinformatics analysis. SS, MJA,
321 and NRJ prepared figures and tables. GK and JHW cultivated and harvested plant
322 specimens used for initial small RNA-seq experiments. NRJ, SS, TP, and MJA
323 cultivated and harvested plant specimens for other experiments. EW, GK, CWD, and
324 JHW performed genome and transcriptome sequencing and preliminary assemblies.
325 FW, SS, and NRJ performed RNA blots. SS and MJA performed 5'-RLM-RACE and
326 qRT-PCR. CC and TP constructed small RNA-seq libraries. NRJ and VB-G performed
327 growth assays. MJA and JHW conceived of the project. MJA wrote and revised the
328 manuscript with input from all other authors.

Author Information

The authors declare no competing financial interests

Correspondence and requests for materials should be addressed to Michael J. Axtell at mja18@psu.edu

337 **Extended Data**

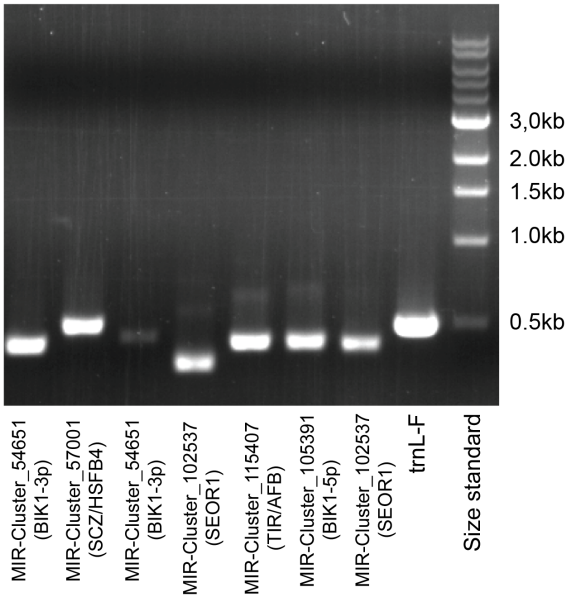

338

339 **Extended Data Figure 1**. PCR of *C. campestris MIRNA* loci. The template for PCR was

340 genomic DNA isolated from *C. campestris* seedlings four days after germination; the

341 seedlings had never attached to nor been near a host plant, ruling out host DNA

342 contamination. trnL-F: Positive control plastid locus.

343

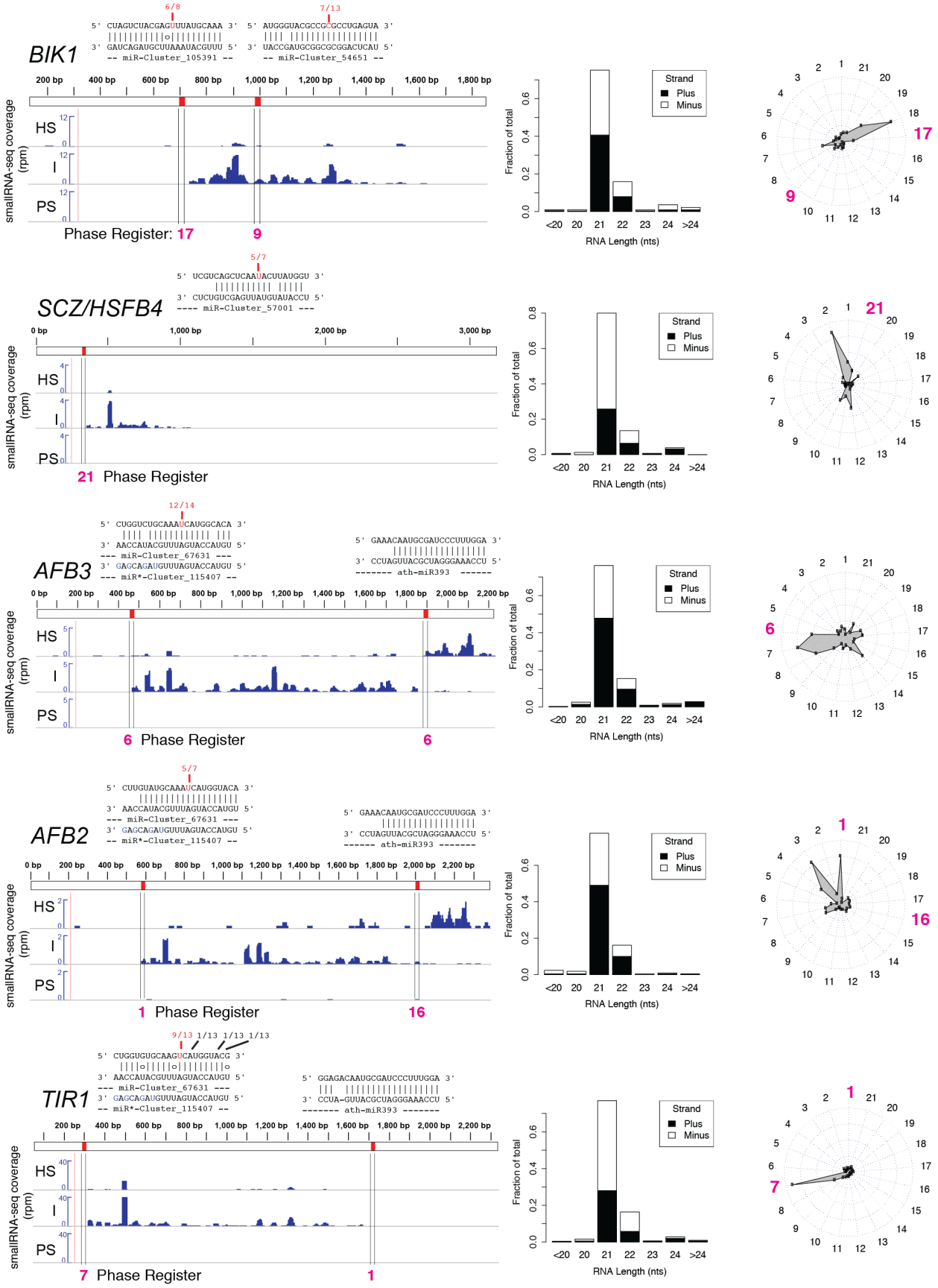
BIK1
6/8
7/13
5' CUAGUCUACGAGUUUAUGCAAA 3'
3' GAUCAGAUGCUUAAAUACGUUU 5'
-- miR-Cluster_105391 --
5' AUGGGUACGCCGCGCCUGAGUA 3'
3' UACCGAUGCGGCGCGGACUCAU 5'
-- miR-Cluster_54651 --
Phase Register: 17 9
SCZ/HSFB4
5/7
5' UCGUCAGCUCAAUACUUAUGGU 3'
3' CUCUGUCGAGUUAUGUAUACCU 5'
---- miR-Cluster_57001 ---
21 Phase Register
AFB3
12/14
5' CUGGUCUGCAAAUCAUGGCACA 3'
3' AACCAUACGUUUAGUACCAUGU 5'
--- miR-Cluster_67631 ---
3' GAGCAGAUGUUUAGUACCAUGU 5'
--- miR*-Cluster_115407 --
5' GAAACAAUGCGAUCCCUUUGGA 3'
3' CCUAGUUACGCUAGGGAAACCU 5'
------- ath-miR393 ------
6 Phase Register 6
AFB2
5/7
5' CUUGUAUGCAAAUCAUGGUACA 3'
3' AACCAUACGUUUAGUACCAUGU 5'
--- miR-Cluster_67631 ---
3' GAGCAGAUGUUUAGUACCAUGU 5'
-- miR*-Cluster_115407 --
5' GAAACAAUGCGAUCCCUUUGGA 3'
3' CCUAGUUACGCUAGGGAAACCU 5'
------ ath-miR393 -------
1 Phase Register 16
TIR1
9/13 1/13 1/13 1/13
5' CUGGUGUGCAAGUCAUGGUACG 3'
3' AACCAUACGUUUAGUACCAUGU 5'
--- miR-Cluster_67631 ---
3' GAGCAGAUGUUUAGUACCAUGU 5'
-- miR*-Cluster_115407 --
5' GGAGACAAUGCGAUCCCUUUGGA 3'
3' CCUA-GUUACGCUAGGGAAACCU 5'
------- ath-miR393 -------
7 Phase Register 1
smallRNA-seq coverage (rpm)
HS
I
PS
Strand
Plus
Minus
Fraction of total
RNA Length (nts)
<20 20 21 22 23 24 >24

345 **Extended Data Figure 2**. *C. campestris* miRNAs cause slicing and phased siRNA
346 production from host mRNAs. Small RNA-seq coverage across the indicated *A. thaliana*
347 transcripts are shown in blue for host stem (HS), interface (I), and parasite stem (PS)
348 samples. For display, the two biological replicates of each type were merged. y-axis is
349 in units of reads per million. Red marks and vertical lines show position of
350 complementary sites to *C. campestris* miRNAs, with the alignments shown above.
351 Fractions indicate numbers of 5'-RLM-RACE clones with 5'-ends at the indicated
352 positions; the locations in red are the predicted sites for miRNA-directed slicing
353 remnants. Bar charts show the length and polarity distribution of transcript-mapped
354 siRNAs. Radar charts show the fractions of siRNAs in each of the 21 possible phasing
355 registers; the registers highlighted in magenta are the ones predicted by the miRNA
356 target sites.
357

Cp_v0.1_Contig11111_02898.1 .. A *TIR/AFB* ortholog

```
5' CUGGUCUGCAAGUCCUGGUACG 3' Transcript: Cp_v0.1_Contig11111_02898.1:82-103 Slice Site:94
   || ||||o|||o|| ||||||o
3' GAGCAGAUGUUUAGUACCAUGU 5' Query: Cluster_115407_miRNA-star

5' CUGGUCUGCAAGUCCUGGUACG 3' Transcript: Cp_v0.1_Contig11111_02898.1:82-103 Slice Site:94
    |||| |||||o|| ||||||o
3' AACCAUACGUUUAGUACCAUGU 5' Query: Cluster_67631_miRNA
```

Cp_v0.1_Contig122651_07831.1 .. A *BIK1* ortholog

```
5' AUGGGUACGCCGCUCCCGAGUA 3' Transcript: Cp_v0.1_Contig122651_07831.1:668-689 Slice Site:680
   |||| |||||||| || |||||
3' UACCGAUGCGGCGCGGACUCAU 5' Query: Cluster_54651_miRNA
```

Cp_v0.1_Contig297862_09445.1 .. A *TIR/AFB* ortholog

```
5' CUGGUCUGCAAGUCCUGGUACG 3' Transcript: Cp_v0.1_Contig297862_09445.1:82-103 Slice Site:94
   || ||||o|||o|| ||||||o
3' GAGCAGAUGUUUAGUACCAUGU 5' Query: Cluster_115407_miRNA-star

5' CUGGUCUGCAAGUCCUGGUACG 3' Transcript: Cp_v0.1_Contig297862_09445.1:82-103 Slice Site:94
    |||| |||||o|| ||||||o
3' AACCAUACGUUUAGUACCAUGU 5' Query: Cluster_67631_miRNA
```

Cp_v0.1_Contig3449_00601.1 ..A *TIR/AFB* ortholog

```
5' CUCGUCUGCAAGUCGUGGUACC 3' Transcript: Cp_v0.1_Contig3449_00601.1:259-280 Slice Site:271
   |||||||o|||o||o||||||
3' GAGCAGAUGUUUAGUACCAUGU 5' Query: Cluster_115407_miRNA-star
```

Cp_v0.1_Contig370259_15766.1 .. An *SCZ/HSFB4* ortholog

```
5' CAGACAGCUCAACACAUACGGG 3' Transcript: Cp_v0.1_Contig370259_15766.1:225-246 Slice Site:237
    |||||||||||| ||||| ||o
3' CUCUGUCGAGUUAUGUAUACCU 5' Query: Cluster_57001_miRNA
```

Cp_v0.1_Contig501179_37185.1 .. An *SCZ/HSFB4* ortholog

```
5' CAGACAGCUCAACACAUACGGG 3' Transcript: Cp_v0.1_Contig501179_37185.1:213-234 Slice Site:225
    |||||||||||| ||||| ||o
3' CUCUGUCGAGUUAUGUAUACCU 5' Query: Cluster_57001_miRNA
```

Cp_v0.1_Contig70142_36225.1 .. An *SCZ/HSFB4* ortholog

```
5' CAGGCAGCUCAACACUUAUGGA 3' Transcript: Cp_v0.1_Contig70142_36225.1:300-321 Slice Site:312
    ||o|||||||| || ||||||
3' CUCUGUCGAGUUAUGUAUACCU 5' Query: Cluster_57001_miRNA
```

Cp_v0.1_Contig81842_24454.1 .. A *BIK1* ortholog

```
5' UUGUAUAUGAAUUUAUGCAGA 3' Transcript: Cp_v0.1_Contig81842_24454.1:608-628 Slice Site:619
   |||| ||||||| o|||||||
3' AACAAAUACUUAUGUACGUCU 5' Query: Cluster_105389_miRNA-star

5' CUUGUAUAUGAAUUUAUGCAGA 3' Transcript: Cp_v0.1_Contig81842_24454.1:607-628 Slice Site:619
   || || ||o||||||||||||o|
3' GAUCAGAUGCUUAAAUACGUUU 5' Query: Cluster_105391_miRNA

5' AAGGCUAUGCUGCCCCUGAGUA 3' Transcript: Cp_v0.1_Contig81842_24454.1:893-914 Slice Site:905
     |||||o||o|| ||||||||
3' UACCGAUGCGGCGCGGACUCAU 5' Query: Cluster_54651_miRNA
```

360 **Extended Data Figure 3.** Possible miRNA target sites within endogenous *C.*

361 *campestris* mRNAs. Note that none of these mRNAs had evidence of any secondary

362 siRNA accumulation, and the complementarity of these sites was generally poor.

363

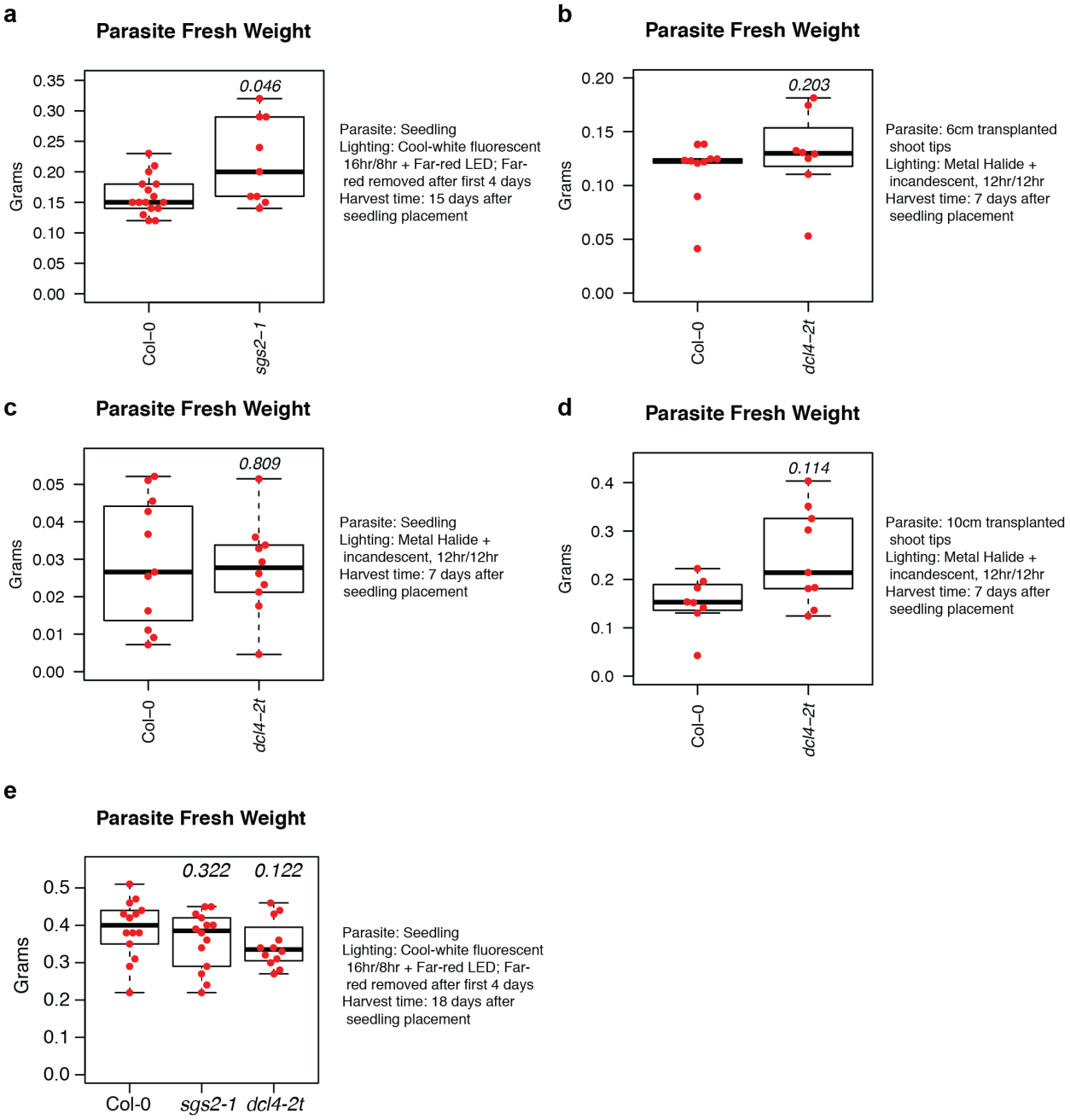

Extended Data Figure 4. Growth of *C. campestris* on *A. thaliana sgs2-1* and *dcl4-2t* mutants with varying methodologies, as indicated. P-values (Wilcoxon rank-sum tests, unpaired, two-tailed) from comparison of mutant to wild-type (Col-0) are shown. Dots show all data points. Boxplots represent medians (horizontal lines), the central half of

369 the data (boxes), and other data out to 1.5 times the interquartile range (whiskers). **a)**
370 n=16 and 9 for Col-0 and *sgs2-1*, respectively. **b)** n=10 and 8 for Col-0 and *dcl4-2t*,
371 respectively. **c)** n=11 and 10 for Col-0 and *dcl4-2t*, respectively. **d)** n=8 and 9 for Col-0
372 and *dcl4-2t*, respectively. **e)** n=14, 14, and 12 for Col-0, *sgs2-1*, and *dcl4-2t*,
373 respectively.
374

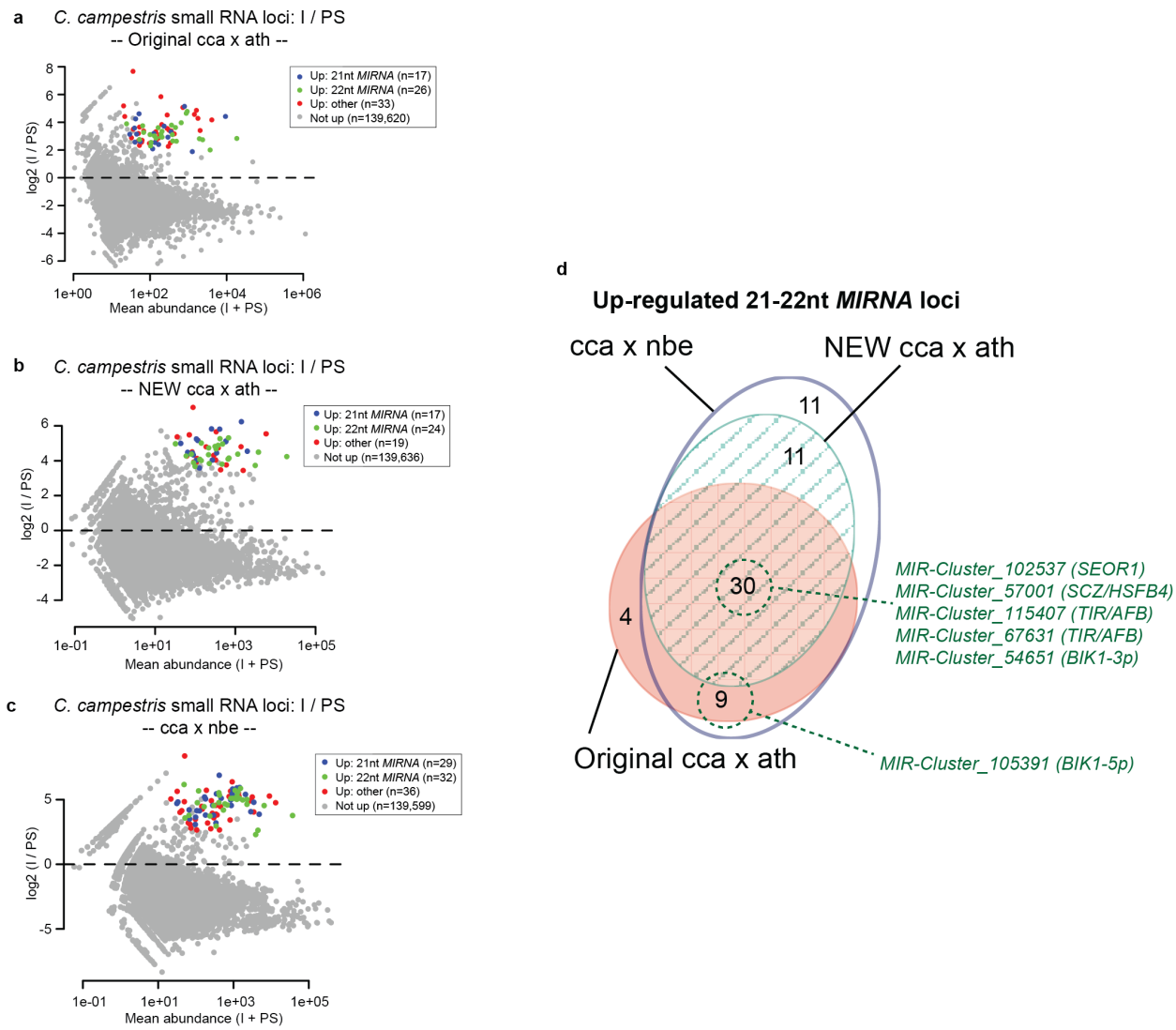

Extended Data Figure 5. Highly reproducible induction of *C. campestris MIRNA*s on different hosts. **a)** MA plot from original experiment on *A. thaliana* hosts of *C. campestris* small RNA loci comparing interface (I) to parasite stem (PS) samples. Significantly up-regulated loci (alternative hypothesis: true difference > 2-fold, FDR <= 0.05) are highlighted. Reproduced from Figure 1A. **b-c)** As in a, except for a new set of *A. thaliana* hosts (b) or from an experiment using *Nicotiana benthamiana* as hosts (c). **d)** Area-proportional Euler diagram showing overlaps of up-regulated *C. campestris* 21-22

384 nt *MIRNA* loci between the three small RNA-seq experiments. The locations of the six

385 *MIRNA* loci of special interest are highlighted in green.

386

387

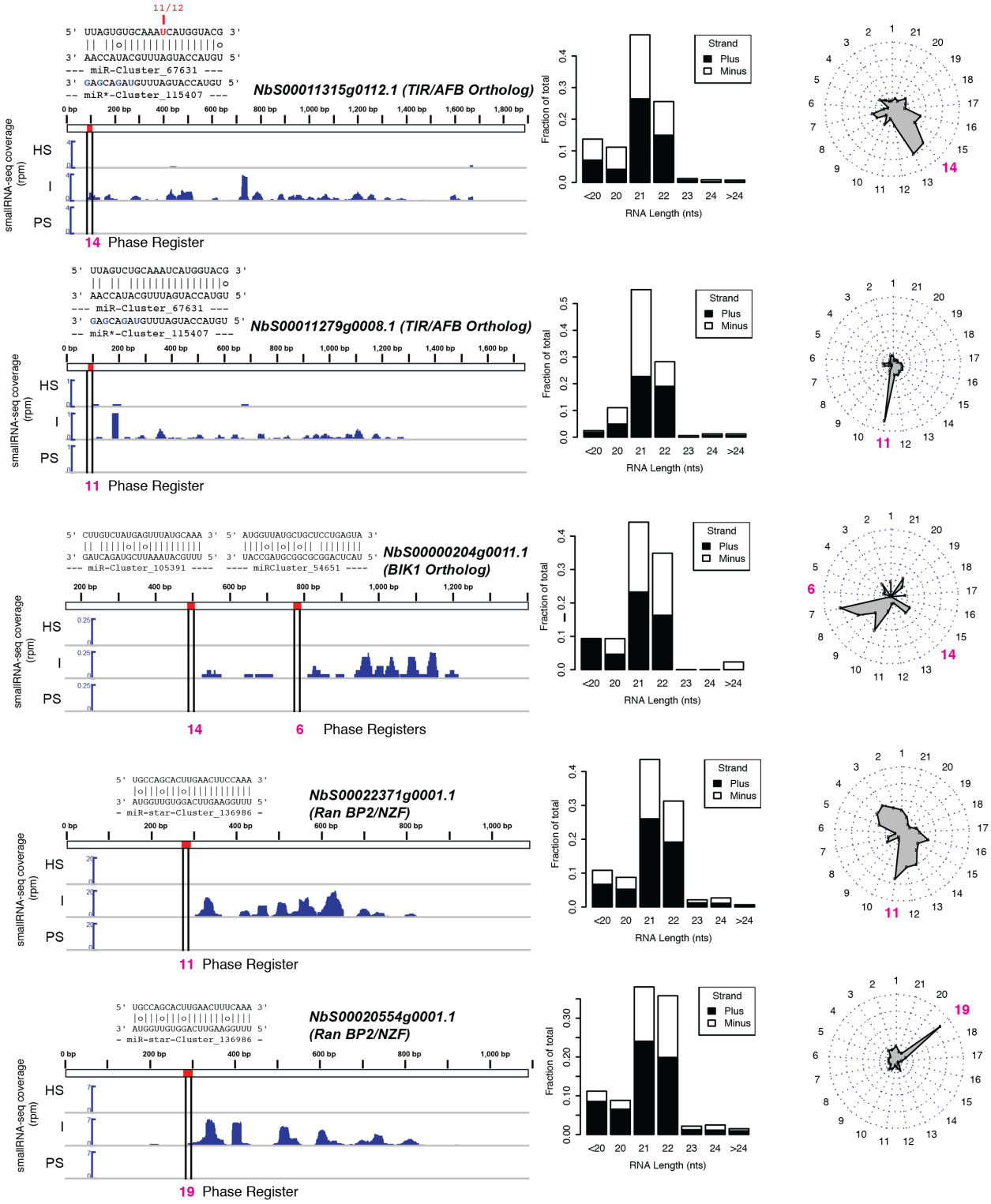
11/12
5' UUAGUGUGCAAAUCAUGGUACG 3'
3' AACCAUACGUUUAGUACCAUGU 5'
--- miR-Cluster_67631 ---
3' GAGCAGAUGUUUAGUACCAUGU 5'
-- miR*-Cluster_115407 ---
NbS00011315g0112.1 (TIR/AFB Ortholog)
smallRNA-seq coverage (rpm)
HS
I
PS
14 Phase Register
Strand
Plus
Minus
Fraction of total
RNA Length (nts)
NbS00011279g0008.1 (TIR/AFB Ortholog)
11 Phase Register
5' CUUGUCUAUGAGUUUAUGCAAA 3'
3' GAUCAGAUGCUUAAAUACGUUU 5'
--- miR-Cluster_105391 ----
5' AUGGUUAUGCUGCUCCUGAGUA 3'
3' UACCGAUGCGGCGCGGACUCAU 5'
---- miRCluster_54651 ----
NbS00000204g0011.1 (BIK1 Ortholog)
14 6 Phase Registers
5' UGCCAGCACUUGAACUUCCAAA 3'
3' AUGGUUGUGGACUUGAAGGUUU 5'
- miR-star-Cluster_136986 -
NbS00022371g0001.1 (Ran BP2/NZF)
11 Phase Register
5' UGCCAGCACUUGAACUUUCAAA 3'
3' AUGGUUGUGGACUUGAAGGUUU 5'
- miR-star-Cluster_136986 -
NbS00020554g0001.1 (Ran BP2/NZF)
19 Phase Register

389 **Extended Data Figure 6**. *C. campestris* miRNAs cause slicing and phased siRNA
390 production from *Nicotiana benthamiana* mRNAs. Small RNA-seq coverage across the
391 indicated *N. benthamiana* transcripts are shown in blue for host stem (HS), interface (I),
392 and parasite stem (PS) samples. For display, the two biological replicates of each type
393 were merged. y-axis is in units of reads per million. Red marks and vertical lines show
394 position of complementary sites to *C. campestris* miRNAs, with the alignments shown
395 above. Fraction indicates numbers of 5'-RLM-RACE clones with 5'-ends at the indicated
396 positions; the locations in red are the predicted sites for miRNA-directed slicing
397 remnants. Barcharts show the length and polarity distribution of transcript-mapped
398 siRNAs. Radar charts show the fractions of siRNAs in each of the 21 possible phasing
399 registers; the registers highlighted in magenta are the ones predicted by the miRNA
400 target sites.
401

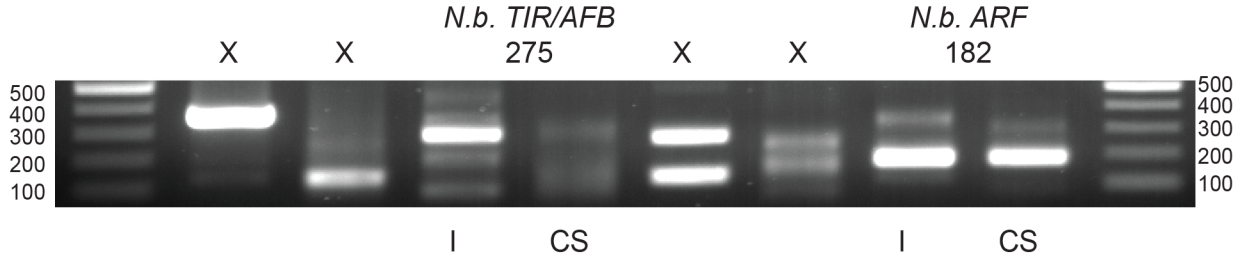

Extended Data Figure 7. Uncropped image of *N. benthamiana* 5'-RLM-RACE products. Lanes with 'X' are irrelevant to this study. This is the uncropped version of the image in Figure 4C.

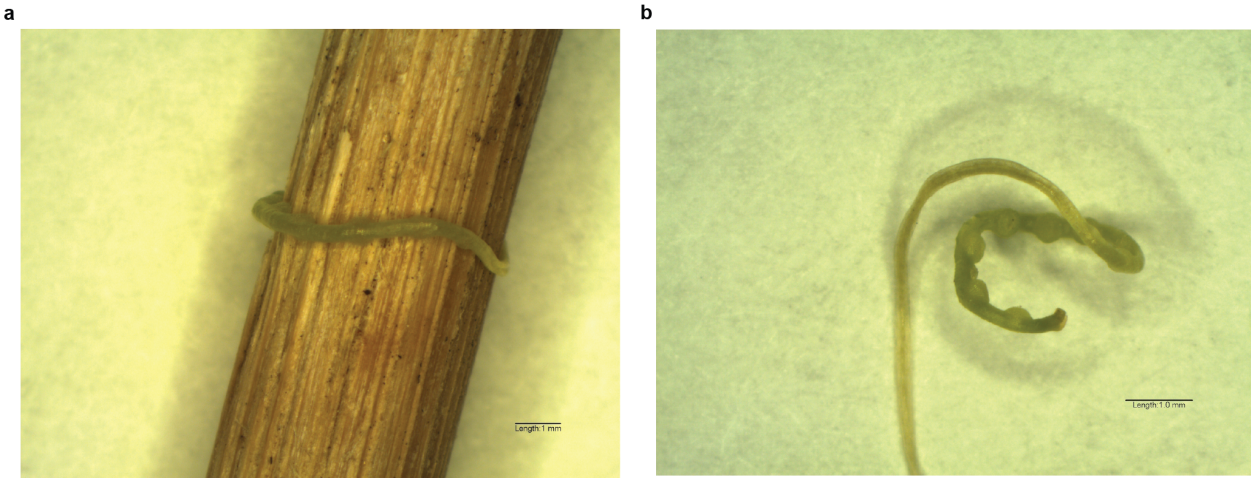

Extended Data Figure 8. *C. campestris* pre-haustoria. **a)** *C. campestris* seedling wound around a bamboo stake. **b)** The same seedling, removed from the stake to show the prominent pre-haustorial bumps. Seedling was scarified, germinated on moist paper towels for three days at ~28C, and then placed next to bamboo stake for four days with far-red LED lighting. Approximately 30 such seedlings were used for the 'PH' RNA in Figure 4B. Scales bars: 1mm.

Phytozome 11 species code	Species	*BIK1*	*SEOR1*	*SCZ / HSFB4*	*TIR1*	*GAPDH*
Org_Acoerulea	*Aquilegia coerulea*	0	1	0	1	0
Org_Alyrata	*Arabidopsis lyrata*	1	1	0	1	0
Org_Athaliana	*Arabidopsis thaliana*	1	1	1	1	0
Org_BrapaFPsc	*Brassica rapa*	1	0	1	1	0
Org_Bstricta	*Boechera stricta*	1	0	0	1	0
Org_Cclementina	*Citrus clementina*	0	1	0	0	0
Org_Cgrandiflora	*Capsella grandiflora*	1	0	0	1	0
Org_Cpapaya	*Carica papaya*	1	0	1	1	0
Org_Crubella	*Capsella rubella*	1	0	0	1	0
Org_Csativus	*Cucumus sativus*	0	0	0	0	0
Org_Csinensis	*Citrus sinensis*	1	1	0	1	0
Org_Egrandis	*Eucalyptus grandis*	0	1	1	1	0
Org_Esalsugineum	*Eutrema salsugineum*	1	0	0	1	0
Org_Fvesca	*Fragaria vesca*	0	NA	NA	1	1
Org_Gmax	*Glycine max*	1	1	1	1	0
Org_Graimondii	*Gossypium raimondii*	1	0	1	1	0
Org_Kmarnieriana	*Kalanchoe marnieriana*	0	1	1	1	0
Org_Lusitatissimum	*Linum usitatissimum*	0	1	0	0	0
Org_Mdomestica	*Malus domestica*	0	NA	0	1	0
Org_Mesculenta	*Manihot esculenta*	1	1	0	1	0
Org_Mguttatus	*Mimulus gattus*	1	NA	0	1	0
Org_Mtruncatula	*Medicago truncatula*	1	1	0	1	0
Org_Ppersica	*Prunus persica*	0	NA	0	1	0
Org_Ptrichocarpa	*Populus trichocarpa*	1	1	1	1	0
Org_Pvulgaris	*Phaseolus vulgaris*	0	1	0	1	0
Org_Rcommunis	*Ricinus communis*	1	1	0	1	0
Org_Slycopersicum	*Solanum lycopersicum*	0	1	1	1	0
Org_Spurpurea	*Salix purpurea*	0	1	1	0	0
Org_Stuberosum	*Solanum tuberosum*	1	NA	1	1	0
Org_Tcacao	*Theobroma cacao*	0	1	1	1	0
Org_Vvinifera	*Vitis vinifera*	0	1	1	1	0

Extended Data Table 1. Predicted miRNA targets un multiple plant species. Targets were predicted using targetdinder.pl, keeping all hits with a score of 4.5 or less. Probable orthologs of the indicated Arabidopsis thaliana genes were found using BLASTP against the 31 eudicot species present in Phytozome 11, simply keeping up to the top 100 BLAST hits. miRNA queries were all mature miRNAs and miRNA*'s from C. campestris interface-induced MIRNA loci. An entry of 'NA' means no probable orthologs were recovered from a given species. A 1 means there was one or more predicted

425 target in that species, a 0 means there were 0 predicted targets. GAPDH orthogroup:

426 negative control.

427

428 **METHODS**

429 **Germplasm**

430 *Cuscuta* was initially obtained from a California tomato field, and seed stocks
431 derived from self-pollination through several generations in the Westwood laboratory.
432 The isolate was initially identified as *Cuscuta pentagona* (Engelm.) *C. pentagona* is very
433 closely related to *C. campestris* (Yunck.), and the two are distinguished by microscopic
434 differences in floral morphology; because of this they have often been confused[1]. We
435 subsequently determined that our isolate is indeed *C. campestris*. *Arabidopsis thaliana*
436 *sgs2-1* mutants[2] were a gift from Hervé Vaucheret (INRA Versailles, France). *A.*
437 *thaliana dcl4-2t* mutants (GABI_160G05[3]) were obtained from the Arabidopsis
438 Biological Resource Center (The Ohio State University, USA). *A. thaliana seor* mutants
439 (GABI-KAT 609F04[4]) were a gift from Michael Knoblauch (Washington State University,
440 USA). The *A. thaliana tir1-1/afb2-* and *afb3*-4 mutants[5] were a gift from Gabriele
441 Monshausen (The Pennsylvania State University, USA). The *bik1* mutant[6] was a gift
442 from Tesfaye Mengiste (Purdue University, USA). The *scz2* mutant[7] was a gift from
443 Renze Heidstra (Wageningen University, The Netherlands). All *A. thaliana* mutants
444 were in the Col-0 background.

445

446 **Growth conditions and RNA extractions**

447 For initial experiments (small RNA-seq and RNA blots in Figure 1) *A.*
448 *thaliana* (Col-0) plants were grown in a growth room at 18-20°C with 12-h light per day,
449 illuminated (200 μmol $m^{-2}s^{-1}$) with metal halide (400W, GE multi-vapor lamp) and spot-
450 gro (65W, Sylvania) lamps. *C. campestris* seeds were scarified in concentrated sulfuric

451 acid for 45 min, followed by 5-6 rinses with distilled water and dried. *C. campestris*
452 seeds were placed in potting medium at the base of four-week-old *A. thaliana* seedlings
453 and allowed to germinate and attach to hosts. The *C. campestris* plants were allowed to
454 grow and spread on host plants for an additional three weeks to generate a supply of
455 uniform shoots for use in the experiment. Sections of *C. campestris* shoot tip (~10 cm
456 long) were placed on the floral stem of a fresh set of *A. thaliana* plants. Parasite shoots
457 coiled around the host stems and formed haustorial connections. Tissues from plants
458 that had established *C. campestris* with at least two coils around healthy host stems and
459 clear parasite growth were used in these studies. Control plants were grown under the
460 same conditions as parasitized plants, but were not exposed to *C. campestris*.
461 For the preparation of tissue-specific small RNA libraries, tissues were harvested
462 after *C. campestris* cuttings had formed active haustorial connections to the host. This
463 was evidenced by growth of the *C. campestris* shoot to a length of at least 10 cm
464 beyond the region of host attachment (7-10 d after infection). Three tissues were
465 harvested from the *A. thaliana*-*C. campestris* associations: 1) 2.5 cm of *A. thaliana* stem
466 above the region of attachment, 2) *A. thaliana* and *C. campestris* stems in the region of
467 attachment (referred to as the interface), 3) 2.5 cm of the parasite stem near the point of
468 attachment. To remove any possible cross-contamination between *A. thaliana* and *C.*
469 *campestris*, harvested regions of the parasite and host stem were taken 1 cm away
470 from the interface region and each harvested tissue was surface cleaned by immersion
471 for 5 min in 70% ethanol, the ethanol was decanted and replaced, the process was
472 repeated three times and the stems were blotted dry with a Kimwipe after the final rinse.
473 All three sections of tissue were harvested at the same time and material from 20

474 attachments were pooled for small RNA extraction. Small RNA was extracted from ~
475 100 mg of each tissue using the mirPremier microRNA Isolation Kit (Sigma-Aldrich, St.
476 Louis, MO, USA) according to the manufacturer's protocol. Small RNA was analyzed
477 using an Agilent small RNA Kit on a 2100 Bioanalyzer platform.

478 Samples used for RNA ligase-mediated 5' rapid amplification of cDNA ends (5'-
479 RLM-RACE; Figure 2D), quantitative reverse-transcriptase polymerase chain reaction
480 (qRT-PCR; Figure 3A) analyses of *A. thaliana* targets were prepared as described
481 above with the following modifications: Col-0 *A. thaliana* hosts were cultivated in a
482 growth room with 16 hr. days, 8 hr. nights, at ~23C, under cool-white fluorescent lamps,
483 attachment of *C. campestris* cuttings was promoted by illumination with far-red LED
484 lighting for 3-5 days, and total RNA was extracted using Tri-reagent (Sigma) per the
485 manufacturer's suggestions, followed by a second sodium-acetate / ethanol precipitation
486 and wash step. Samples used for RNA blots of secondary siRNA accumulation from *A.*
487 *thaliana* mutants and replicate small RNA-seq libraries were obtained similarly, except
488 that the samples derived from the primary attachments of *C. campestris* seedlings on
489 the hosts instead of from cuttings. In these experiments, scarified *C. campestris*
490 seedlings were first germinated on moistened paper towels for three days at ~28C, then
491 placed adjacent to the host plants with their radicles submerged in a water-filled
492 0.125ml tube.

493 *C. campestris* pre-haustoria (Extended Data Figure 8) were obtained by
494 scarifying, germinating and placing seedlings as described above, next to bamboo
495 stakes in soil, under illumination from cool-white fluorescent lights and far-red emitting
496 LEDs. Seedlings coiled and produced pre-haustoria four days after being placed, and

497 were harvested and used for total RNA extraction (used for RNA blot in Figure 4B)
498 using Tri-reagent as described above. *Nicotiana benthamiana* was grown in a growth
499 room with 16 hr. days, 8 hr. nights, at ~23C, under cool-white fluorescent lamps. Three-
500 to four-week old plants served as hosts for scarified and germinated *C. campestris*
501 seedlings. Attachments were promoted by three-six days with supplementation by far-
502 red emitting LEDs. Under these conditions, *C. campestris* attached to the petioles of the
503 *N. benthamiana* hosts, not the stems. Interfaces and control petioles from un-
504 parasitized hosts were collected 7-8 days after successful attachments, and total RNA
505 (used for RNA blots in Figure 4B and small RNA-seq libraries) recovered using Tri-
506 reagent as described above.
507
508 **small RNA-seq**
509 The initial small RNA-seq libraries were constructed using the Illumina Tru-Seq
510 small RNA kit per the manufacturer's protocol and sequenced on an Illumina HiSeq2500
511 instrument. Subsequent small RNA-seq libraries (replicate two using *A. thaliana* hosts,
512 and the *N. benthamiana* experiments) instead used New England Biolabs NEBnext
513 small RNA library kit, following the manufacturer's instructions. Raw sRNA-seq reads
514 were trimmed to remove 3'-adapters, and filtered for quality and trimmed length >= 16
515 nts using cutadapt[8] version 1.9.1 with settings "-a TGGAATTCTCGGGTGCCAAGG --
516 discard-untrimmed -m 16 --max-n=0". For experiments where *A. thaliana* was the host,
517 trimmed reads that aligned with zero or one mismatch (using bowtie[9] version 1.1.2,
518 settings "-v 1") to the *A. thaliana* plastid genome, the *C. gronovii* plastid genome (*C.*
519 *gronovii* was the closest relative to *C. campestris* that had a publically available

520 completed plastid genome assembly available), *A. thaliana* rRNAs, tRNAs, snRNAs, or
521 snoRNAs were removed. Similarly, for experiments where *N. benthamiana* was the
522 host, the reads were cleaned against the *C. gronovii* plastid genome, the *N. tabacum*
523 plastid genome and rRNAs, and a set of tRNAs predicted from the *N. benthamiana*
524 genome using tRNAscanSE.

525 For the original *A. thaliana* host data, the 'clean' reads were aligned and
526 analyzed with reference to the combined TAIR10 *A. thaliana* reference genome and a
527 preliminary version 0.1 draft genome assembly of *C. campestris* using ShortStack[10]
528 (version 3.8.3) using default settings. The resulting annotated small RNA loci
529 (Supplementary Data 1) were analyzed for differential expression (I vs. PS) using
530 DESeq2[11], with a $\log_2$ fold threshold of 1, alternative hypothesis of "greaterAbs", and
531 alpha of 0.05. p-values were adjusted for multiple testing using the Benjamini-Hochberg
532 procedure, and loci with an adjusted p-value of <= 0.05 (equivalent to an FDR of <=
533 0.05) were called up-regulated in I relative to PS. Among the up-regulated loci, those
534 annotated by ShortStack as *MIRNA*s deriving from the *C. campestris* genome which
535 produced either a 21nt or 22nt mature miRNA (Supplementary Data 2) were retained
536 and further analyzed. The predicted secondary structures and observed small RNA-seq
537 read coverage was visualized (Supplementary Data 3-4) using strucVis (version 0.3;
538 https://github.com/MikeAxtell/strucVis).

539 For analysis of mRNA-derived secondary siRNAs, the 'clean' small RNA-seq
540 reads from the original *A. thaliana* experiment were aligned to the combined TAIR10
541 representative cDNAs from *A. thaliana* and our preliminary version 0.1 transcriptome
542 assembly for *C. campestris*, using ShortStack[10] version 3.8.3, with settings --

543 mismatches 0, --nohp, and defining the full length of each mRNA as a 'locus' using
544 option --locifile. The resulting counts of small RNA alignments for each mRNA were
545 used for differential expression analysis, comparing I vs. HS, using DESeq2 [11] as
546 described above. *A. thaliana* mRNAs with significantly up-regulated (FDR <= 0.05)
547 small RNAs comparing I vs. HS were retained for further analysis. The cDNA
548 sequences of these loci were retrieved, and used for miRNA target predictions using
549 GSTAr (version 1.0; https://github.com/MikeAxtell/GSTAr); the full set of mature
550 miRNAs and miRNA*'s (Supplementary Data 2) from the I-induced *C. campestris*
551 *MIRNA* loci were used as queries.

552 Analysis of the second set of *A. thaliana* - *C. campestris* small RNA-seq data
553 aligned the cleaned reads to the combined *A. thaliana* and *C. campestris* reference
554 genomes as described above, except that the list of loci derived in the analysis of the
555 original data (Supplementary Data 1) was used as a "--locifile" in the ShortStack
556 analysis. Differential expression analysis was then performed using DESeq2 as
557 described above. Analysis of the *N. benthamiana* - *C. campestris* small RNA-seq data
558 began with a ShortStack analysis of the cleaned reads against the combined *N.*
559 *benthamiana* (version 0.4.4) genome and the preliminary assembly of the *C. campestris*
560 genome, using default settings. The *de novo N. benthamiana* loci obtained from this run
561 were retained. The resulting alignments were used to quantify small RNA abundance
562 from the *C. campestris* small RNA loci defined with the original data. The resulting read
563 counts were then used for differential expression analysis with DESeq2 as described
564 above. Analysis of secondary siRNAs derived from *N. benthamiana* mRNAs was
565 performed similarly as the *A. thaliana* mRNA analysis described above, except that the

566 combined transcriptomes were from *C. campestris* and *N. benthamiana* (version 0.4.4
567 annotations).
568
569 **RNA blots**
570 Small RNA gel blots were performed as previously described[12] with
571 modifications. For the blots in Figure 1B, small RNAs (1.8 micrograms) from each
572 sample were separated on 15% TBE-Urea Precast gels (Bio-Rad), transblotted onto the
573 Hybond NX membrane and cross-linked using 1-ethyl-3-(3-dimethylamonipropyl)
574 carbodiimide[13]. Hybridization was carried out in 5×SSC, 2×Denhardt's Solution, 20 mM
575 sodium phosphate (pH 7.2), 7% SDS with 100 µg/ml salmon testes DNA (Sigma-
576 Aldrich). Probe labeling, hybridization and washing were performed as described[12].
577 Radioactive signals were detected using Typhoon FLA 7000 (GE Healthcare).
578 Membranes were stripped in between hybridizations by washing with 1% SDS for 15
579 min at 80°C and exposed for at least 24 h to verify complete removal of probe before re-
580 hybridization. Sequences of probes are listed below. Blots in Figures 3B and 4B were
581 performed similarly, except that 12 micrograms of total RNA were used instead. Probe
582 sequences are listed in Supplementary Data 6.
583
584 **5' RNA ligase-mediated rapid amplification of cDNA ends (5'-RLM-RACE)**
585 Five micrograms of total RNA were ligated to one microgram of a 44 nucleotide
586 RNA adapter (Supplementary Data 6) using a 20ul T4 RNA ligase 1 reaction (NEB) per
587 the manufacturer's instructions for a one-hour incubation at 37C. The reaction was then
588 diluted with 68ul of water and 2ul of 0.5M EDTA pH 8.0, and incubated at 65C for 15

589 minutes to inactivate the ligase. Sodium acetate pH5.2 was added to a final
590 concentration of 0.3M, and the RNA precipitated with ethanol. The precipitated and
591 washed RNA was resuspended in 10ul of water. 3.33ul of this sample was used as the
592 template in a reverse transcription reaction using random primers and the Protoscript II
593 reverse transcriptase (NEB) per the manufacturer's instructions. The resulting cDNA
594 was used as template in first round PCR using a 5' primer matching the RNA adapter
595 and a 3' gene-specific primer (Supplementary Data 6). 1ul of the first round PCR
596 product was used as the template for nested PCR with nested primers (Supplementary
597 Data 6). Gene-specific primers for *A. thaliana* cDNAs were based on the representative
598 TAIR10 transcript models, while those for *N. benthamiana* cDNAs were based on the
599 version 0.4.4 transcripts (Sol Genomics Network[14]). In Figure 4c, *N. benthamiana*
600 *TIR/AFB* is transcript ID *NbS00011315g0112.1*; *N. benthamiana ARF* is transcript ID
601 *NbS00059497g0003.1*. Bands were gel-purified from agarose gels and cloned into
602 pCR4-TOPO (Life Tech). Inserts from individual clones were recovered by colony PCR
603 and subject to Sanger sequencing.
604
605 **Quantitative reverse-transcriptase PCR (qRT-PCR)**
606 Total RNA used for qRT-PCR was first treated with DNaseI (RNase-free; NEB)
607 per the manufacturer's instructions, ethanol precipitated, and resuspended. 2
608 micrograms of treated total RNA was used for cDNA synthesis using the High Capacity
609 cDNA Synthesis Kit (Applied Biosystems) per the manufacturer's instructions. PCR
610 reactions used PerfeCTa SYBR Green FastMix (Quanta bio) on an Applied Biosystems
611 StepONE-Plus quantitative PCR system per the manufacturer's instructions. Primers

612 (Supplementary Data 6) were designed to span the miRNA target sites, to ensure that
613 only uncleaved mRNAs were measured. Three reference mRNAs were used: *ACTIN*,
614 *PP2A (PP2A sub-unit PDF2*; *At1g13320*), and *TIP41-l* (*TIP41-like; At4g34270*) [15]. Raw
615 Ct values were used to calculate relative normalized expression values to each
616 reference mRNA separately, and the final analysis took the median relative expression
617 values between the *ACTIN*- and *TIP41-l* normalized data.
618
619 ***C. campestris* growth assays**
620 *C. campestris* seedlings were scarified, pre-germinated, and placed next to hosts
621 in 0.125ml water-filled tubes under cool-white fluorescent lighting supplemented with
622 far-red emitting LEDs (16hr day, 8hr night) at ~ 23C as described above. After a single
623 attachment formed (4 days), far-red light supplementation was removed to prevent
624 secondary attachments. After 18 more days of growth, entire *C. campestris* vines were
625 removed and weighed (Figure 3C). Multiple additional growth trials were performed
626 specifically on the *dcl4-2t* and *sgs2-1* mutant hosts under varying conditions (Extended
627 Data Figure 4).
628
629 **miRNA target predictions**
630 To find probable orthologs for *Arabidopsis thaliana* genes of interest, the *A.*
631 *thaliana* protein sequences were used as queries for a BLASTP analysis of the 31
632 eudicot proteomes available on Phytozome 11
633 (https://phytozome.jgi.doe.gov/pz/portal.html#). Transcript sequences for the top 100
634 hits were retrieved. In some cases no hits from a particular species were found; these

635 are 'N/A' on Figure 4a. The miRNA query set was all mature miRNAs and miRNA*s
636 from the I-induced, *C. campestris*-derived 21nt or 22nt *MIRNA*s (Supplementary Data
637 2). Targets were predicted from the probable 31-species with a maximum score of 4.5
638 using targetfinder.pl (https://github.com/MikeAxtell/TargetFinder/) version 0.1.
639 *N. benthamiana* orthologs of *A. thaliana* proteins were found based on BLAST-P
640 searches against the version 0.4.4 *N. benthamiana* protein models at Sol Genomics
641 Network[14], and miRNA target sites predicted using targetfinder.pl as above.

642 **Code availability**

643 ShortStack[10] (small RNA-seq analysis), strucVis (visualization of predicted RNA
644 secondary structures with overlaid small RNA-seq depths), and
645 Shuffler.pl/targetfinder.pl (prediction of miRNA targets controlling for false discovery
646 rate) are all freely available at https://github.com/MikeAxtell. Cutadapt version 1.9.1[8] is
647 freely available at http://cutadapt.readthedocs.io/en/stable/index.html. The R package
648 DESeq2[11] is freely available at http://www.
649 bioconductor.org/packages/release/bioc/html/DESeq2.html.
650

651 **Data Availability**

652 Small RNA-seq data from this work are available at NCBI GEO under accession
653 GSE84955 and NCBI SRA under project PRJNA408115. The draft, preliminary *C.*
654 *campestris* genome and transcriptome assemblies used in this study are available at
655 the Parasitic Plant Genome Project website at http://ppgp.huck.psu.edu.
656

657 **References (Methods)**

658 1. Costea, M., García, M. A., Baute, K. & Stefanović, S. Entangled evolutionary
659 history of Cuscuta pentagona clade: A story involving hybridization and Darwin in
660 the Galapagos. *Taxon* **64,** 1225–1242 (2015).
661 2. Elmayan, T. *et al.* Arabidopsis mutants impaired in cosuppression. *Plant Cell* **10,**
662 1747–1758 (1998).
663 3. Xie, Z., Allen, E., Wilken, A. & Carrington, J. C. DICER-LIKE 4 functions in trans-
664 acting small interfering RNA biogenesis and vegetative phase change in
665 Arabidopsis thaliana. *Proc Natl Acad Sci USA* **102,** 12984–12989 (2005).
666 4. Froelich, D. R. *et al.* Phloem ultrastructure and pressure flow: Sieve-Element-
667 Occlusion-Related agglomerations do not affect translocation. *Plant Cell* **23,**
668 4428–4445 (2011).
669 5. Parry, G. *et al.* Complex regulation of the TIR1/AFB family of auxin receptors.
670 *Proc Natl Acad Sci USA* **106,** 22540–22545 (2009).
671 6. Veronese, P. *et al.* The membrane-anchored BOTRYTIS-INDUCED KINASE1
672 plays distinct roles in Arabidopsis resistance to necrotrophic and biotrophic
673 pathogens. *Plant Cell* **18,** 257–273 (2006).
674 7. Hove, ten, C. A. *et al.* SCHIZORIZA encodes a nuclear factor regulating
675 asymmetry of stem cell divisions in the Arabidopsis root. *Curr Biol* **20,** 452–457
676 (2010).
677 8. Martin, M. Cutadapt removes adapter sequences from high-throughput
678 sequencing reads. *EMBnet. journal* (2011).
679 9. Langmead, B., Trapnell, C., Pop, M. & Salzberg, S. L. Ultrafast and memory-
680 efficient alignment of short DNA sequences to the human genome. *Genome Biol*

681 **10,** R25 (2009).
682 10. Johnson, N. R., Yeoh, J. M., Coruh, C. & Axtell, M. J. Improved Placement of
683 Multi-Mapping Small RNAs. *G3 (Bethesda)* (2016). doi:10.1534/g3.116.030452
684 11. Love, M. I., Huber, W. & Anders, S. Moderated estimation of fold change and
685 dispersion for RNA-seq data with DESeq2. *Genome Biol* **15,** 550 (2014).
686 12. Cho, S. H., Coruh, C. & Axtell, M. J. miR156 and miR390 regulate tasiRNA
687 accumulation and developmental timing in Physcomitrella patens. *Plant Cell* **24,**
688 4837–4849 (2012).
689 13. Pall, G. S. & Hamilton, A. J. Improved northern blot method for enhanced
690 detection of small RNA. *Nat Protoc* **3,** 1077–1084 (2008).
691 14. Bombarely, A. *et al.* A draft genome sequence of Nicotiana benthamiana to
692 enhance molecular plant-microbe biology research. *Mol Plant Microbe Interact* **25,**
693 1523–1530 (2012).
694 15. Czechowski, T., Stitt, M., Altmann, T., Udvardi, M. K. & Scheible, W.-R. Genome-
695 wide identification and testing of superior reference genes for transcript
696 normalization in Arabidopsis. *Plant Physiol* **139,** 5–17 (2005).
697
698

SI Guide

Supplementary Data 1: *A. thaliana* and *C. campestris* small RNA loci. Output from ShortStack 3.8.3 (https://github.com/MikeAxtell/ShortStack) showing all small RNA loci identified in this study. (.xlsx format)

Supplementary Data 2: Mature miRNAs and miRNA*s from *C. campestris* Interface-induced *MIRNA* loci. (.xlsx format)

Supplementary Data 3: Details of *C. campestris MIRNA* loci: Text-based sequences, predicted secondary structures, and aligned small RNA reads (all six libraries). Lower-case letters indicate small RNA bases that are mismatched to the genomic sequence. Plain-text (ASCII) format.

Supplementary Data 4: Images showing *C. campestris* hairpins overlaid with color-codes representing total read-depth (all six 'original' *C. campestris* x *A. thaliana* small RNA libraries). (pdf, 43 pages).

Supplementary Data 5: Alignments of mature miRNAs and miRNA*s (from Supplementary Data 2 -- the induced *C. campestris* miRNAs) against the *A. thaliana* genome. Note that most have three or more mismatches. (SAM format).

Supplementary Data 6: Oligonucleotide sequences. Excel (.xlsx) format.